ENHANCED COMPACTION OF STRESSED NORTH SEA CHALK DURING WATERFLOODING

Mark A. Andersen
Amoco Production Company, Tulsa, OK

Abstract The high porosity chalk found in North Sea petroleum reservoirs is mechanically very weak; in many cases there is little or no cementation. When placed under high stress it compacts significantly. The material obeys a rate-type compaction model which is based on friction between the coccolith fragments. In this model, after the material exceeds its yield point many of the particles in contact are subject to almost enough shear force to overcome frictional resistance to motion.

Compaction tests were performed on material for which the native saturation was preserved before testing. The initial water saturation was about 5%. The material was constrained in a uniaxial-strain condition before and during waterflooding. Prior to waterflooding with simulated sea water, the material was allowed to creep for several days. Contacting the chalk with water effects a substantial additional compaction immediately after the water is introduced to the sample. The results clearly indicate that localized compaction follows the water front through the sample. The effect was easily seen on plastic material (stress above the yield point), but was negligible in elastic (pre-yield) material.

The water-induced compaction was about 1% bulk strain (for plastic material) occurring over a six-day period after water injection. However, after waterflooding the sample requires a larger-than-normal increase in stress before compaction begins again. The net result after a large increase in stress beyond the water front passage is that the compaction is the same as if the mate-

rial had not been waterflooded. The long-term effect on produced oil is small, but changes in permeability in the water flooded zone may be experienced in the field.

INTRODUCTION

Chalk from the North Sea oil fields can have very high porosity and can be mechanically weak. Porosity up to 50% has been reported, with pore collapse stresses as low as 500 psi and pore-volume compressibility in excess of 15/GPA (100 x 10^{-6}/psi) (Ruddy et al. 1989). The primary production potential from the rock drive is enormous, but without an active water drive, substantial amounts of oil remain after primary production. A pilot waterflood is underway in the Valhall Field to evaluate the waterflood potential.

In the early phases of production, there were indications of a chalk-water interaction. The material failed at a lower stress when saturated with brine than when saturated with oil (Botter 1985). Tests on Ekofisk Field chalk (Rhett 1990, Monjoie et al. 1990) indicate a rapid compaction when brine contacts the chalk, under certain conditions, but no effect under other conditions. Finding the cause of this water-induced compaction is important for confident engineering of a waterflood.

The high porosity chalk from the Tor Formation of Valhall Field obeys a rate-type compaction model (Andersen et al. 1992). This friction-based model provides insight into the mechanism underway when waterflooding chalk. The interplay between interfacial forces at the waterfront and the failure mechanism explains the water-induced compaction seen in the laboratory studies.

RATE-DEPENDENT CHALK COMPACTION MECHANISM

The microstructure of the weak North Sea chalks is fundamentally different from the microstructure of conventional reservoir materials. It is important to keep this basic difference in mind when examining the mechanical behavior of these materials. The scanning electron micrograph in the top of Figure 1 shows grains of a cemented sandstone magnified to 235x. These grains are about the size of beach sand. The pore spaces are the dark zones, and each is surrounded

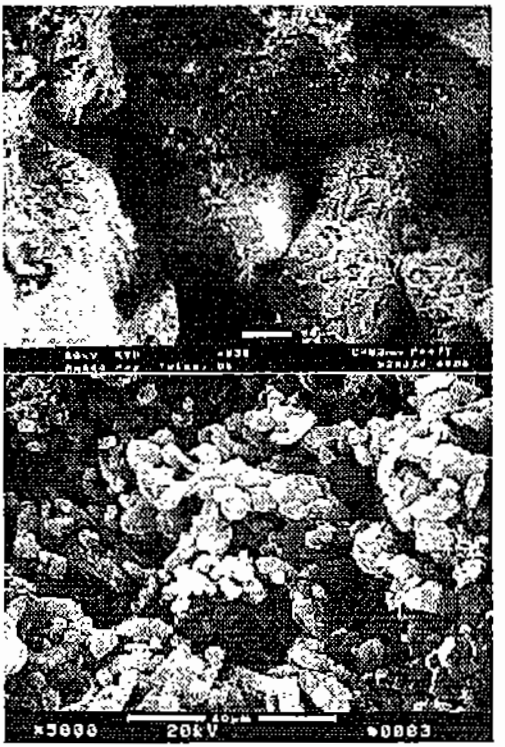

FIGURE 1. Upper: Scanning Electron Microscope image of sandstone at 235x. Lower: Scanning Electron Microscope image of North Sea chalk at 5000x.

by only a few sand grains. Each of the grains acts as a strong "beam" which together form a relatively strong support structure protecting the pore space from increases in net overburden stress. As formation fluid is produced, more of the overburden weight is shifted to the support structure. There may be some reorientation of grains and some breaking of cemented contacts, but for most sandstone reservoirs there is little effect on the pore volume. The pore-volume compressibility is small (0.4 to 0.7/GPA, 3 to 5 x 10^{-6}/psi), and the axial shortening is about a percent of the material length over stress

changes of interest in a formation.

The lower electron micrograph in Figure 1 shows a North Sea chalk magnified to 5000x. The chalk particles (coccoliths) are about the size of dust. Although the pore spaces are very small, they make up almost 50% of the volume of the material. It is not the scale of the particle size which affects the mechanical behavior of interest here. Rather it is that each pore is protected by "beams" and "arches" made up of many chalk particles, and that the particles are very poorly cemented. In Valhall Field, the Tor Formation chalk is about 97-99% calcite. These "beams" are not nearly so strong as the single grain "beams" supporting the sandstone pore structure. When the pore pressure in chalk is reduced by hydrocarbon production, the load shifted to the chalk structure exceeds the ability of these weak "arches" to support it, and the chalk fails.

The rate-type compaction model (de Waal 1986) is ideally suited for a material with no cementation (Andersen et al. 1992). It does not explain the shape of the pore-volume collapse curve; that is determined by the strength of the cementation and the porosity (Botter 1985). Instead it is a theory which explains the dynamic effects in such a material. For example, the amount of compaction depends on the rate at which the material is loaded. The compaction observed in the laboratory is less than the compaction expected in the field, where the same stress state is achieved at a much slower rate of loading. Figure 2 shows the data from the laboratory tests, performed at 0.1% strain/hour, and the extrapolation to the field rate of 0.0001% strain/hour (Andersen et al.). Similar curves can be obtained for other rates of strain in between these two by interpolation. The curves are approximately parallel, fanning out from a common yield stress. Porosity log measurements from closely-spaced wells indicate the porosity decline in the field matches this behavior (Halvorsen 1991).

The vertical portions of the curves of the laboratory data in Figure 2 are creep tests performed under constant vertical net stress. Each creep test is followed by a nearly horizontal portion, having low pore-volume and bulk compressibility, termed the overconsolidated region. These represent regions of stress which came to some equilibrium at a loading rate lower than the rate being applied during the measurement. Here the material is able to support the imposed rate of loading without failure. At a stress point defined by the rate-type model, the material again compacts more rapidly. The curve defined

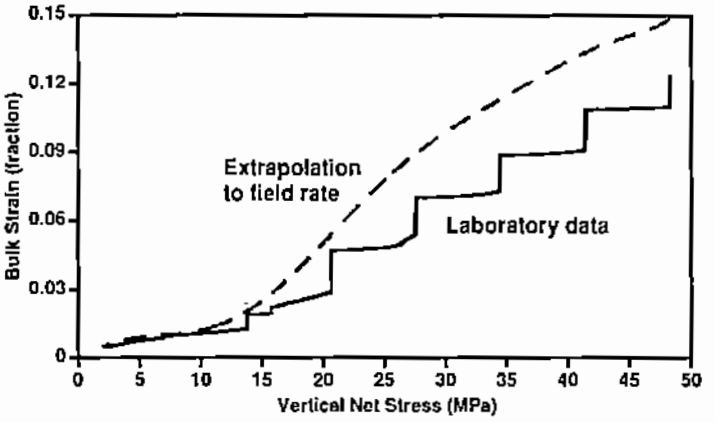

FIGURE 2. Laboratory data and extrapolation to field rate from rate-type model.

by the material at the imposed loading rate of 0.1%/hour is termed the virgin compaction curve at 0.1%.

The behavior of the material during the creep test is also explained by the rate-type theory. After a short period of time, the creep increases linearly with the logarithm of elapsed time. The creep data in the upper part of Figure 3 is indistinguishable from the model fit. In the lower plot, the creep rate is shown. Note that the model fit at the beginning of the creep test is very close to the imposed 0.1%/hour strain rate preceding the creep. The large fluctuations in creep rate at times beyond 5000 minutes represent permeability measurements. The rate-type theory explains both the long-time logarithmic behavior and the short time transient behavior. The creep data are used with the model to predict the field-rate compaction (Andersen et al. 1992).

RATE-DEPENDENT EFFECTS ARE FRICTION BASED

The basis of the theory is the assumption that the dynamic effects are dependent on the material's resistance to movement, that is, the

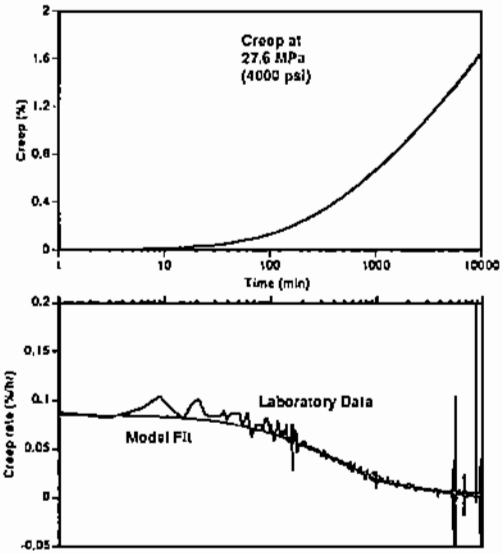

FIGURE 3. Upper plot: the model overlaps the chalk data. Lower plot: model predict creep rate data.

frictional properties of the intergranular contact. With little to no cementation, the only resistance to movement can be friction. Up to the yield point, the friction between particles exceeds the shear force at the grain contacts resulting from the applied stress. Note that even in hydrostatic loading, some grain-to-grain contacts can be under shear loading. The yield point is the stress condition at which a significant number of grain contacts can no longer support the shear loading and they move, or break between particles. At least some of these moving particles were part of the support structure around the "large" pores, and so a substantial local reduction in pore space occurs.

Another aspect of this failure is a cascade effect. In any particular volume of chalk, there are a few "arches" or "beams" which support more load than their neighbors. These are likely the first to fail either through breaking the collection of chalk particles, or by sliding across the base on which the support rests. When this support fails,

the load which it bore is shifted to neighboring "arches" and "beams". If some of them are near to failure, the load shift may cause them to fail, resulting in an expanding zone of failure. Once the applied stress exceeds the chalk yield stress, much of the material is metastable - at or near to the shear stress needed to overcome friction. This regional failure has been seen in other studies (Rhett and Teufel 1991).

When the material is unloaded by decreasing the net stress, or in the field by increasing the pore pressure, it behaves quasi-elastically. The compressibility is very low, closer to a conventional formation compressibility than to the compressibility of the failed chalk material. This is consistent with the microscopic picture of rate-dependent failure. Unloading the material decreases the shear force at the grain contacts, decreasing the propensity for motion and failure and making it more stable.

The permeability decline in these samples is small in relationship to the large volume loss. Most samples retain about 1/3 of the low stress permeability when the applied stress reaches 48.3 MPa (7000 psi). Mercury injection data in Figure 4 shows that for companion samples, the pore throat diameter changes only from about 1.1 micron to about 0.8 micron as a result of compaction to 48.3 MPa. Since the pore throats are about the size of a grain, movement of aggregates of particles will not decrease the pore throat size much, even though the pore volume is decreasing significantly.

WATER-INDUCED CHALK COMPACTION

With the understanding of the microscopic failure mechanism provided by the rate-type model, the water-induced compaction can be explained. It is first necessary to understand some basic aspects of interfacial tension and wettability.

The Valhall Field Tor Formation chalk is neutral to oil-wetting: the Amott-Harvey wettability index in Valhall Tor ranges from 0 to -0.37. With an in-situ water saturation of about 5%, water is probably not a continuous phase in this chalk. The water which is injected during the waterflood is the non-wetting phase intruding into the material. The capillary pressure, which is the difference between the pressure in the wetting phase (P_w) and the nonwetting phase (P_{nw}) at the flood front, is given by the relation in Table 1, where $\gamma\cos\theta$ is the

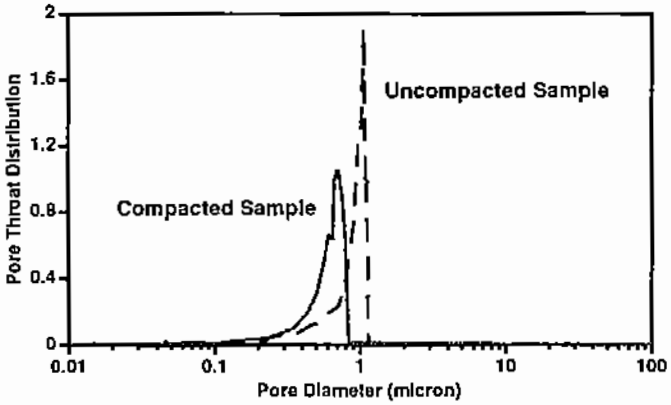

FIGURE 4. Pore throat distribution from mercury injection test on companion samples, before and after compaction.

adhesion tension and r_t is the radius of the constriction (pore throat) at the flood front. The interfacial tension of recombined Valhall crude as measured against sea water at reservoir temperature is 35 dyne/cm, with a water-advancing contact angle of about 150°. The adhesion tension is 30 dyne/cm. Mercury injection indicates the largest pore throats are about 1 micron in diameter (Figure 4). The capillary pressure at the largest pore throats is then 1.2×10^6 dyne/cm^2 (120 kPa, 17.4 psi).

At an interface such as that depicted schematically in Figure 5, the pressure in the water phase is 17.4 psi greater than the pressure in the oil phase. The column of chalk particles which separates the phases is exposed to a shear force of this pressure difference multiplied by the area exposed to the pressure difference. The photomicrograph on which this figure is based indicates structures of 10-20 one-micron particles. The force on such a 4 particle x 4 particle structure would be about 0.2 dyne (Table 1). This value can be compared with the average force normal to a grain-to-grain contact in this chalk. With a 50% porosity (Φ), the average particle occupies twice its volume, and so twice its cross-section. At a vertical stress of 20.7 MPa (3000 psi) (somewhat lesser horizontal stress), the

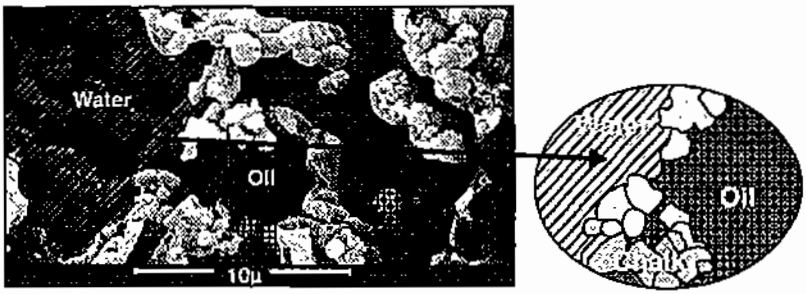

FIGURE 5. Schematic representation of water displacing oil in chalk with low initial water saturation. The blow-up to the right illustrates the interface where water intrudes into a pore throat.

average force/particle in the major stress direction is 3.25 dyne. Although this is an average normal force, the shear forces and the frictional resistance will be of the same order. The factor of 16 between the interfacial force and the shear force is small in comparison with the values for a conventional sandstone.

Table 1 shows the similar forces in a sandstone. The shear force acts on each grain, giving a larger force on sandstone than on chalk due to the larger sand grain size. However, the normal force is much larger, so a waterflood has little effect on sandstone.

The basis of the rate-type compaction model is friction-controlled grain motion. Consider what happens when a localized shear event, such as a water front, moves through such a metastable material. Grain contacts experiencing almost enough shear force already will, if the direction of shear is right, be given a "shove" by the passage of the meniscus. This support structure will fail, beginning a local cascade as neighboring supports take up the load. If there is no preferred grain orientation, the cascading failure will occur both parallel to and perpendicular to the direction of the flood front. One interesting aspect of this effect is that it is localized to the flood front. The passage of the meniscus is a triggering event for the cascading failure. Behind the front, there is no additional drive force to keep the population of moving grain contacts constant, so it will decay in the same fashion as the stress-induced compaction decay seen in the

TABLE 1. Shearing forces due to wetting

$$P_c = P_{nw} - P_w = \frac{2\gamma\cos\theta}{r_t} \quad \text{(EQ 1)}$$

$$WettingShear = P_c \times AreaofStructure \quad \text{(EQ 2)}$$

$$NormalForce/particle = \frac{Stress \times AreaofGrain}{1-\Phi} \quad \text{(EQ 3)}$$

	r_t	Area of Grain	Area of Structure	Capillary Pressure	Welting Shear	Force/ particle
	μm	μm x μm	μm x μm	dyne/cm^2	dyne	dyne
Sandstone	25	100 x 150	100 x 150	2.4×10^4	3.6	1.2×10^5
Chalk	0.5	1 x 1	4 x 4	1.2×10^6	0.2	3.2

constant stress creep tests. As the flood front moves, so does the zone of greatest compaction.

CONSTANT STRAIN-RATE TESTS WITH CREEP

The equipment used for the laboratory tests is described in Andersen et al. (1992) and Ruddy et al. (1989). The measurements were performed under strain-rate control, except during creep tests, which were under constant vertical stress control. Uniaxial-strain conditions (no lateral deformation) were maintained at all times. The tests were performed at room temperature with injection of room temperature fluids. The fluid was delivered using a 2MPa GDS digital pressure controller with a 1kPa resolution. Each sample was instrumented with two vertical and two horizontal strain gauges, bonded to the chalk. The sample length was monitored using two LVDTs measuring the end piston separation. The arrangement is illustrated in Figure 6. The combination of LVDTs measuring the sample length and gauges monitoring strain at the middle of the sample allows some discrimination of the effect of water on the sample.

The samples were tested without cleaning, with water saturation

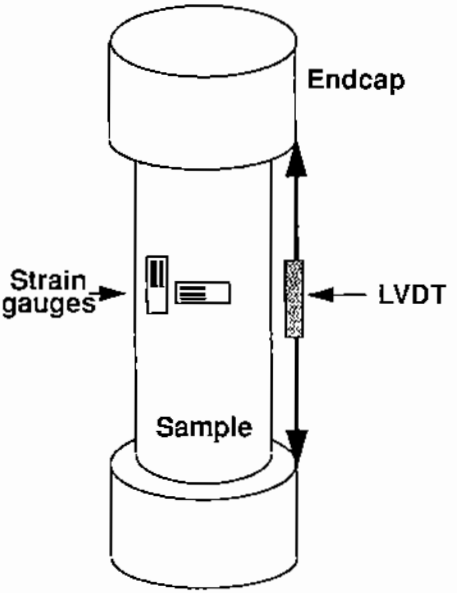

FIGURE 6. Schematic of core assembly showing placement of strain measurements.

of 0-10%. Crude oil was miscibly displaced with a 9.7 cp refined oil before starting the stress test.

The mechanical and creep properties were determined by increasing the load at a rate of 0.1% strain/hour. This rate was selected to avoid pore-pressure buildup, which was monitored throughout the test and is negligible. At each 6.9 MPa (1000 psi), the vertical stress was held constant and a creep test of 3 or more days duration was performed. The waterflooding was done after a creep period of five days at 27.5 MPa (4000 psi) (Sample 7) or 13 days at 20.6 MPa (3000 psi) (Sample 8). One sample was waterflooded at low confining stress (pre-yield). That sample showed no effect of water on the mechanical properties of the material. Below the yield stress, the material is stable to small shearing forces.

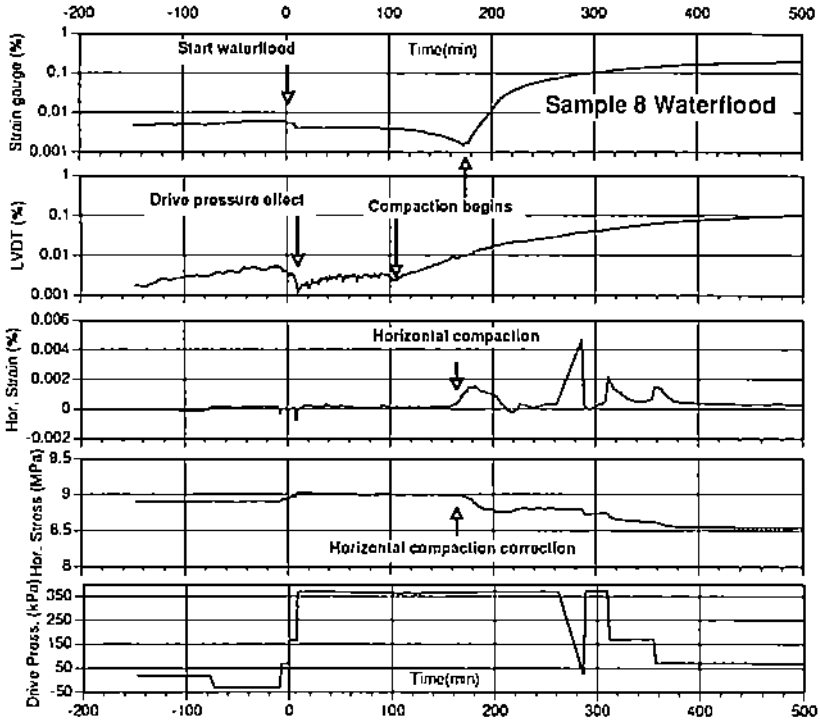

FIGURE 7. Stress and strain results from waterflooding chalk.

MATERIAL COMPACTION DURING WATERFLOODING

Results from Sample 8 (Figure 7) show the changes in measured quantities during the waterflood. This figure shows the strain at the midpoint; the change of sample length (from LVDT); the horizontal strain; the change in horizontal stress; and the drive pressure. The vertical strain values are strain changes during the waterflood - the zero point is arbitrary; and they are plotted on a logarithmic scale to emphasize the small changes at the start of the waterflood.

When the drive pressure first increases (about 360 kPa, 50 psi), there is a response at both the LVDT and strain gauges, due to the

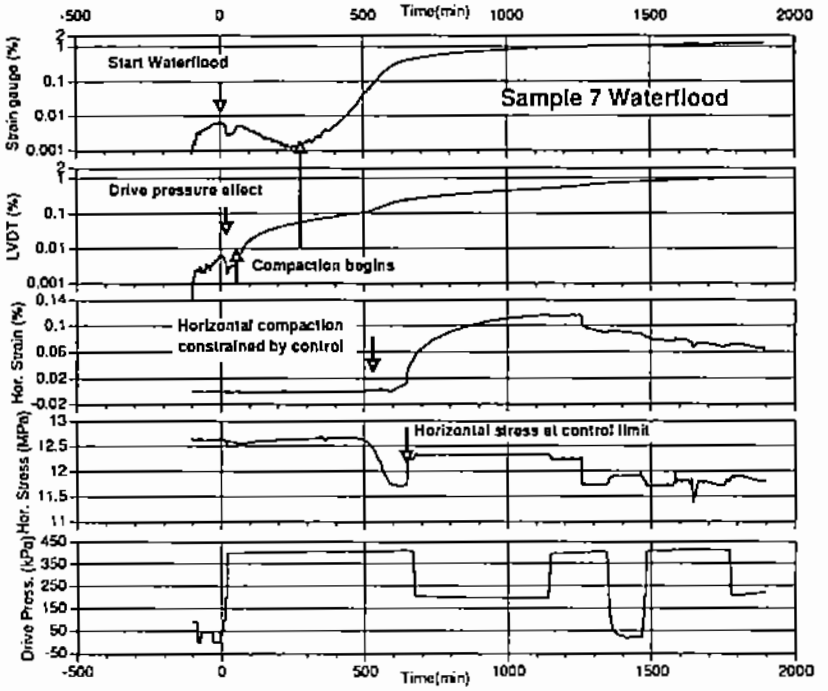

FIGURE 8. Stress and strain results from waterflooding chalk. Control failed when flood front reached horizontal strain gauge.

decrease in net effective stress. This is not a water-induced effect, since the tubing upstream of the chalk is filled with oil which has to be displaced before the water reaches the chalk. The chalk then compacts slightly, a continuation of the creep prior to fluid injection. When the brine reaches the face of the chalk, there is a slight extension recorded on the LVDTs. This could be buildup of water at the face of the core before capillary pressure builds up enough in the water phase to intrude the pore space.

There is a rapid contraction of the material length after the water invades the chalk. This continues for the three days of flooding and three days of continued creep thereafter. The behavior is similar to

the loading-induced creep, in the form of the creep vs. the logarithm of time. The midpoint strain gauges indicate a slow expansion of the material "far" ahead of the waterfront. This continues for about an hour, when the waterfront reaches the midpoint strain gauges and a rapid contraction begins. The fluid throughput when the midpoint strain gauge registers a change is 14% of the pore volume of the first half of the sample. At about this same time, the horizontal strain gauges indicate a compaction in the horizontal direction. This is compensated by the system by decreasing the confining stress, allowing the material to expand back to its original diameter.

The main points of this behavior are also evidenced in Sample 7 (Figure 8): rapid contraction of the sample length when the water reaches the face, with expansion of the midpoint until the water reaches that point. Fluid throughput when the midpoint gauge registers a compaction is about 21% of the pore volume of the first half of the sample. The horizontal strain control was lost during the waterflood, because the horizontal compaction exceeded the set limits of the stress control at about 650 minutes after waterflooding began.

These results illustrate the interfacial- and friction-controlled compaction model. The separate measurements of sample length and point strain at the midpoint of the sample show that the compaction is localized to the water flood front. The response in the horizontal strain gauges shows the material is trying to compact in all directions.

The midpoint strain gauge indicates expansion in advance of the flood front. When the material at the flood front compacts the rest of the material unloads slightly. The implications for this are discussed briefly below in the field conditions section.

After the waterflood, Sample 8 was allowed to continue creeping for several days. The compaction behavior was the same as that observed during a standard creep test, a decay of creep rate with the logarithm of time (Figure 9). This indicates the mechanism of water-induced compaction is fundamentally similar to the loading-induced compaction.

The loading was continued to higher stresses after the waterflood test. Just as with the creep tests, there was a region of stress increase which had low compressibility - the overconsolidated region. Eventually enough additional stress is imposed to force the material back onto the virgin compaction curve defined by the

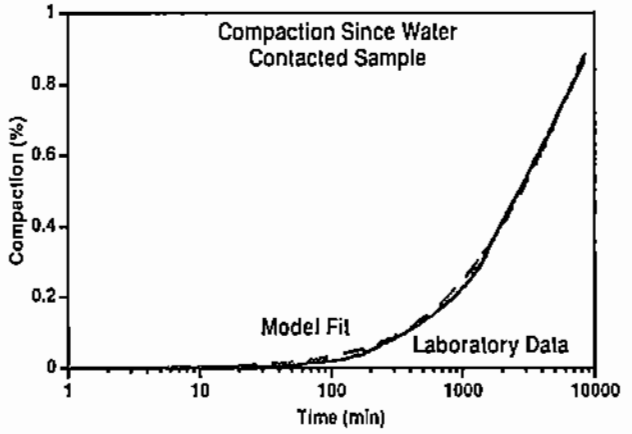

FIGURE 9. The water-induced creep fits the form of the rate-type model.

imposed loading rate of 0.1%/hour. The water-induced compaction has an effect only until the net stress increases beyond the overconsolidated region (Rhett 1990). In Figure 10 the extrapolation to field rate of Sample 6 (Andersen et al. 1992) is compared with the extrapolation for Sample 8. In the curve for Sample 8, the extrapolation between 20.6 and 27.5 MPa (3000 and 4000 psi) is based on the creep test prior to the waterflood. It fits smoothly into the extrapolation of the post-waterflood data. The remarkable agreement in the field rate compaction between these companion samples shows that the waterflood affects the material only until enough additional stress has been added to put the material back onto the virgin compaction curve.

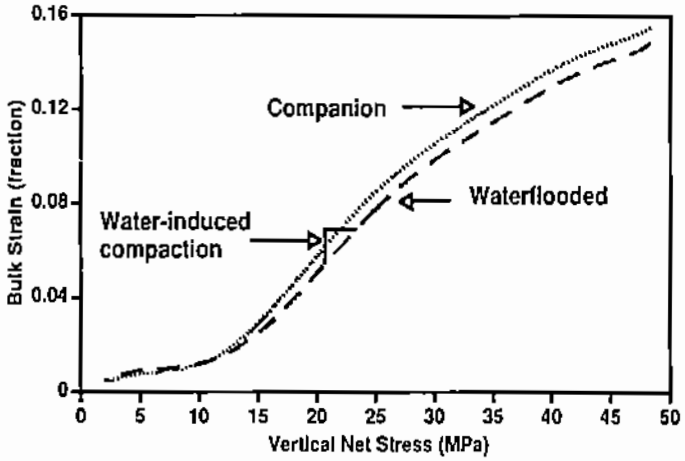

FIGURE 10. The effect of the waterflood is erased by continued pressure decline.

For each of the chalk samples flooded, two effluent samples were collected and tested for calcium content. Calcium dissolves into the simulated seawater, as shown in Table 2, but the amount of dissolution cannot explain the pore volume loss.

TABLE 2. : Calcium content in floodwater

	Concentration (mg/l)	
	Fluid Sample 1	Fluid Sample 2
Injection water	460	460
Sample 7	680	530
Sample 8	730	420

APPLICATION TO FIELD CONDITIONS

The chalk mechanics tests were done in a uniaxial-strain mode. This is appropriate for thin, horizontal, deeply buried formations (Geertsma 1957). In the chalk formation, the boundary conditions in the vicinity of the water front are probably not uniaxial-strain.

Based on the results of the laboratory study, the following picture of a waterflood in this chalk is proposed. Ahead of the flood front, the material is compacting according to the virgin compaction behavior at the field-imposed loading rate. For the high porosity Valhall Field Tor Formation chalk, this could be a compressibility as high as 15/GPa (100 $x10^{-6}$/psi) (Ruddy et al. 1989). However, if the pressure in the formation is increasing due to the water injection, the material could have the very low compressibility of the unloading phase. At the water front, the material compacts even more rapidly, on the order of a percentage or two in sample dimension within a few days. It is not possible to define a "compressibility" in this phase since the compaction is not stress controlled, and in fact was measured at constant stress. However, in the time scale of field compaction events, the water-induced compaction rate is enormous. Behind the flood front, the material is stronger, in the low compressibility over-consolidated region.

The boundary condition near the waterfront in the formation is more like a protected arch than a load-bearing member. The material encompassing the flood front (inches to a few feet) is supported by the stronger material ahead of and behind the flood. Yet the material is decreasing in volume - the only way for the material to compact when the space it occupies is held rigid by the surrounding material is for it to fracture, probably on a very small spacing. One effect would be to enhance the permeability in the waterflooded zone. There are indications from pressure transient tests in a water injection well that this has occurred in the field.

An issue of importance for a field waterflood is the impact of the chalk-water interaction near the wellbore. There have been no indications of chalk weakening at the pilot injection well or at the producing well which has experienced water breakthrough. The laboratory tests and the model suggest that the water-induced compaction is speeding up a process already underway - the stress-induced compaction of the chalk. At the injector well, the water-induced compaction occurs at a time when the near-well formation

pressure is increasing due to the injection. As discussed above, the chalk has a lower compressibility and greater stability on unloading than under loading conditions. However, step changes in injection pressure or injection rates may occur due to compaction-induced fracturing. At the producing well, one must maintain similar precautions when the water breaks through as one does when bringing one of the chalk wells on line after a shut-in. Rapid changes in bottomhole pressure can induce near-well failure and should be avoided.

SPLASHING COLD WATER ON A HOT FORMATION

Some field observations of compaction and cracking in the chalk have been attributed to thermal effects. Cold injection water is pumped into a hot formation, cooling it and inducing thermal cracking. However, the magnitude of change due to thermal cracking is smaller than the water-induced compaction. Assuming a linear thermal expansion coefficient of 2.8×10^{-6}/°C (5×10^{-6}/°F), and a 83°C (150°F) change in temperature, the volumetric change would be about 0.2% due to cooling. The change due to the interface passage is on the order of 1%. Both effects are probably active, and both effects are in the direction of compacting the material. Both should be included in a complete model.

COMPARISON WITH OTHER CHALK WATERFLOOD TESTS

Two other waterflood tests have been reported in the literature on North Sea chalk, both on Ekofisk chalk. Rhett (1990) waterflooded cleaned chalk which had no water and reports rapid compaction when the water reaches the sample. In contrast, chalk which had been cleaned and restored to a low (7-20%) water saturation displayed no additional compaction upon waterflooding. Huegas and Charlez (1990) examined fresh-state chalk which had been flushed with oil for several days, and report rapid compaction when the injected water reaches the chalk.

The fresh state and cleaned, water-free samples are similar to the results reported here, assuming the fresh-state cores are not water-wetting. In both cases, the injection of water would involve passage of a meniscus through the material, which induces the

compaction. The cleaned and restored material is different, in both effect of water injection (none), and wetting state. Once cleaned, the material was first exposed to brine, then desaturated either by flushing to 15-20% water saturation or by vacuum desaturation to 7.5% (Rhett, personal communication 1991). The brine would be in contact with the chalk. When the material is flooded, the meniscus of the type described here would not form. The waterflood would be an imbibition process, not an injection of a nonwetting fluid.

The shearing mechanism proposed by Rhett and Teufel (1991) does not apply to the small changes in net stress used in these laboratory tests. Sample 6 from that study is most like the high porosity, low silica chalk from this study. Their Sample 6 failed in extension rather than shear, suggesting the high porosity material does not fail in the same manner as the lower porosity material.

CONSIDERATIONS OF IMPORTANCE FOR RATE-SENSITIVE MATERIALS

Rate-sensitive effects have been seen in other materials, such as sandstone (de Waal and Smits 1986), diatomite and calcium carbonate (Hamilton and Shafer 1991) and other chalks (Smits et al. 1986; Monjoie et al. 1990). Loading these materials at rates of importance for engineering (field depletion rates) is not generally practical. The technique used here provides an excellent means of extrapolating to field conditions.The rate-type theory (de Waal 1986) is easier to apply to a constant strain-rate test than to a constant stress-rate test. A constant strain-rate test also provides insight into the overconsolidated region which a constant stress-rate test does not (Andersen et al. 1992).

Extrapolation to engineering rates can be done in reasonable detail by performing numerous creep tests. Once the behavior for a given material has been defined, the number of creep tests can be decreased to two or possibly one. In the case of chalk, creep tests near the yield point indicate the yield point is relatively insensitive to the loading rate. Virgin curves at different loading rates are approximately parallel curves, fanning out from a (roughly) common yield stress (Figure 2).

CONCLUSIONS

1. Passing a water meniscus through oil-wet chalk results in compaction of the chalk.
2. The compaction is due to the interfacial forces and the weak bonding inherent in the rate-sensitive material.
3. Material should be tested with native saturations and wettability.
4. Waterfloods in conjunction with strain-rate controlled tests and creep tests give a complete picture which can be extrapolated to field conditions.
5. Boundary conditions during the waterflood tests should be constant volume rather than uniaxial strain.

ACKNOWLEDGEMENTS

I thank Amoco Production Company and Amoco Norway Oil Company and its partners, Amerada Hess Norge A.S., Enterprise Oil Norge Ltd., and Elf Aquitaine Norge A.S. for permission to publish this paper. I also thank Niels Foged and Helle F. Pedersen of the Danish Geotechnical Institute, who acquired the data.

REFERENCES

ANDERSEN, M. A., FOGED, N., PEDERSEN, H. F. (1992). The Rate-type Compaction of a Weak North Sea Chalk. In *Proceedings of the 33rd US Rock Mechanics Symposium*, (Santa Fe 8-10 June 1992), edited by J. R. Tillerson and W. R. Wawersik, pp. 253-261. Rotterdam: A.A. Balkema

BOTTER, B. J. (1985). Pore Collapse Measurements on Chalk Cores. In *North Sea Chalk Symposium* (Stavanger 21-22 May 1985)

DE WAAL, J. A., SMITS, R. M. M. (1985). Prediction of Reservoir Compaction and Surface Subsidence: Field Application of a New Model. *SPE preprint 14214* presented at the 1985 SPE Annual

Technical Conference and Exhibition (Las Vegas 22-25 September 1985)

DE WAAL, J. A. (1986). On the Rate Type Compaction Behavior of Sandstone Reservoir Rock. *Ph.D. thesis*, Delft University.

GEERTSMA, J. (1957). The Effect of Fluid Pressure Decline on Volumetric Changes of Porous Rocks. *Trans. AIME*, 210, 331-340

HALVORSEN, HUGO (1991). Porosity Reduction as a Function of Pressure Depletion in a High Porosity Chalk Field. *M. S. Thesis*, Rogaland University, Stavanger, Norway

HAMILTON, J. M., SHAFER, J. L. (1991). Measurement of Pore Compressibility Characteristics in Rock Exhibiting "Pore Collapse" and Volumetric Creep. *The Society of Core Analysts Annual Technical Conference Preprints*, 3 (San Antonio August 21-22, 1991)

MONJOIE, A., SCHROEDER, C., PRIGNON, P., YERNAUX, C., DA SILVA, F., DEBANDE, G. (1990). Establishment of Constitute Laws of Chalk and Long Term Tests. *Third North Sea Chalk Symposium* (Copenhagen 11-12 June 1990)

RHETT, DOUGLAS W. (1990). Long Term Effects of Water Injection on Strain in North Sea Chalks. *Third North Sea Chalk Symposium* (Copenhagen 11-12 June 1990)

RHETT, D. W., TEUFEL, LAWRENCE W. (1991). Water injection-induced shear fracturing in the Ekofisk Field. *Rock Mechanics as a Multidisciplinary Science, Proceedings of the 32nd U. S. Symposium on Rock Mechanics,* (Norman 10-12 July 1991), edited by J-C Roegiers, pp. 241-250. Rotterdam: A.A. Balkema

RUDDY, I., ANDERSEN, MARK A., PATTILLO, P. D., BISHLAWI, M., FOGED, N. (1989). Rock Compressibility, Compaction and Subsidence in a High Porosity Chalk Reservoir: A Case Study of Valhall Field. *J. Petroleum Tech.* 41(7), 741-746

SMITS, R. M. M., DE WAAL, J. A., VAN KOOTEN, J. F. C. (1986). Prediction of Abrupt Reservoir Compaction and Surface Subsid-

ence Due to Pore Collapse in Carbonates. *SPE preprint 15642* presented at the 1986 SPE Annual Technical Conference and Exhibition (New Orleans 5-8 October 1986)

CONVERSION FACTOR

psi = 6.895 kPa = 0.006895 MPa
dyne/cm = mN/m
dyne/cm^2 = 0.1 n/m^2 = 0.1 Pa